TEST Engineering & Management

January-February 2020
ISSN: 0193-4120 Page No. 12952 - 12959

Quantum Effiency of Tigan/Gan Quantum Dot Sollar Cells with Varying of Environment Temperature

Samir. M. Abdalmohsin
Department of Physics, College of Sciences, Thi-Qar University, Thi-Qar, Iraq

Article Info
Volume 82
Page Number: 12952 - 12959
Publication Issue:
January-February 2020

Article History
Article Received*: 18 May 2019*
Revised*: 14 July 2019*
Accepted*: 22 December 2019*
Publication*: 24 February 2020*

Abstract:
This work deals with thallium-based quantum dot solar cells. The structures studied are *TlGaN*/GaN Structure. The parameters such as energy sub bands, absorption, and quantum efficiency (QE) spectra studied for different temperatures. Found that the absorption intensity and QE were increased with increase of the Our environment Temperature 260,270,300,320,340 K respectively . In addition, QE was decreased with increasing the junction depth for the structures; the proposed solar cells are covering the ultra violet and part of visible range 380-440nm, which have important applications especially in solar cells.

Keywords*: Quantum dotes ,heterojunction ,Solar cells.*

INTRODUCTION

Short wavelength UV (SWUV) devices have a large area of applications extending to space solar cells, convert solar energy to electricity in short wavelength. In this atmospheric window (200-400) nm, the emitted energy density was low while the atmospheric absorption is high. A extensive series of Quantum dotes solar cell (QDSC) technology are studied and researched presently. These days, there exists a strong attempt aimed to build up the third generation QdsSCs. This involve the utilize of nanostructure quantum dots (QDs) as active materials absorber [1]. QDs semiconductor in recent times involved important consideration due to their quantum dotes size effect [2]. QDs have a quantum property like to pure atoms; which create the discrete energy levels [3]. Currently, most important attention was focus on III-V groups of table periods compounds due to their particular optoelectronic properties, like high quantum efficiency gain, have soaring absorption coefficient in the ultraviolet, and visible in regions of the solar spectrum [4]. Among them, the TIGaN is a chemical compound that has the formula Thallium Gallium Nitrite [2]. An III-V semiconductor has priority in the SWUV and visible regions. TIGaNhas high mechanical properties, thermally stability , best dopants, good Substrate and their epitaxial growth techniques. These uniqueness are connected to The covalent bond, which is very strong in semiconductors materials[1]. TIGaN shows the high band gap, it barely covers the 300 to 440 nm wavelength range [4]. Additionally, it suffers from the lack of substrate that can lattice matched with it only GaN gives encouraging results, its band gap enough to cover the SWUV spectrum [2]. To extending wavelength from ultraviolet to visible spectrum, introduces difficulty in miscibility lighter and strengthening indium [3,4].Thallium- structures are very talented in range of SWUV spectrum [5]. The band gap of TlGaN semiconductor was about 2.9 eV, which is appropriate the lattice mismatch in the devices. In addition, TlGaN can be tailored over the whole range of ultraviolet and part of visible spectrum with little possibility to lattice matching with other kind of semiconductor [6]. It has a direct bandgap with all range of semiconductor possible composition. This direct bandgap makes it the main substituent of silicon solar cells [7]. It is a semiconductor of electricity, and It has high

January-February 2020
ISSN: 0193-4120 Page No. 12952 - 12959

electron mobility, and little electron concentration.[8] III-nitrides is broad direct band gap semiconductor materials with soaring thermal and chemical stable semiconductors. The possibility make TIGaN of 2.65-2.9eV bandgap with GaN of 3.50-3.51eV malty layer can produce group to cover broad range of wavelengths .They be able to provide high efficiency of solar cells [9], [10]. Further expansion can be made by adding element with a heaver atomic number like Tl [11]. The study explain that the linear band gap reduce with increase doping of Ti element to structure . [12]. The wurtzite (W) mode find as the structure at ground stable of (TlN) [13].great electronic properties are provided due to the carrier confinement principle [14]. A wide applications for using thallium nanostructures , related to create subband of their energy states. The quantized property of nanoscales have attractive characteristics like high efficiency , changeable wavelength with reduce size particles [15]. QDs was significant in extending the wavelength to the require spectrum in SWUV application. Therefore, Ti base QDs absorb wide spectrum include most part UV ,and short part of visible ,so its very appropriate for solar solar cells application.[15, 16].The research deal with thallium-based QD solar cells. This structure is investigated as a modern and novel structure. The absorption,energy, and QE spectrum are drowning with different temperatures environment spectrum. High QE was obtained associated with high absorption, which decreases with the junction depth until 1 micrometer then increase exponentially. For **QE** Structures with low absorption spectrum, the QE degrease slightly with increasing the junction depth. QE increase with increase the environment temperature. The structure studied covers the 300-440 nm UV and part visible wavelength range

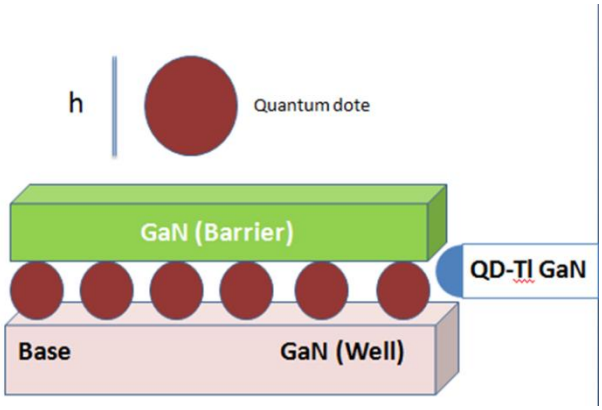

Fig1. Schematic illustration of the QD active layer, which consists of QD arrays grow a WLThe shape represents the layers of Quantum dots solar cell where the ball represent the elements TlGaN QDs

QUANTUM EFFICIENCY IN QUANTUM Dots SOLAR CELLS:

The equation of minority carrier connection among the junctions when the insertion is low levels for the positive charge in p-type side and negative charge in the n-type side , can be written as follow [14]:

$$D_p \frac{\partial^2 \delta p_n}{\partial x^2} - \frac{\delta p_n}{\tau_p} + G_L = 0 \qquad (1)$$

$$D_n \frac{\partial^2 \delta n_p}{\partial x^2} - \frac{\delta n_p}{\tau_n} + G_n = 0 \qquad (2)$$

Where electron concentration which created as result to apply of excitations as expressed in the following $\delta p_n = p_n - p_{n0}$ $(\delta n_p = n_p - n_{p0})$ with $p_n(n_p)$ is the total positive charge in the n-region (p-region), and $p_{n0}(n_{p0})$ is the positive charge density without external insertion. $\tau_p(\tau_n)$ is the hole diffusion length or life time. The speed of electron-hole production which changing with the distance is given by $G(x) = G_L$ [14]

$$G_n = (1-R)\alpha_n \Phi \times \exp\{-(\alpha_n x_j + \alpha_d W + \alpha_p [x - x_j - W])\} (3)$$

January-February 2020
ISSN: 0193-4120 Page No. 12952 - 12959

R is the reflectivity of semiconductor, $\alpha(x)$ is the absorption coefficient of light power, and Φ is the number of photon ,and $\alpha_p, \alpha_n, \alpha_d$ are the absorption coefficients of p-, n-, and depletion layers, respectively. x_j is the depth of depletion , and W is the width of depletion . Eqs. (1) and (2) are solved by summing the homogeneous and particular solutions.

The equation of the hole number per unit area is given by [16], the solve of Equation . (1) is

$$\delta p_n = \frac{\alpha_n \phi(1-R)\tau_p}{(\alpha_n^2 L_p^2 - 1)} \left\{ \frac{\cosh(x/L_p)}{\sinh(x_j/L_p)} \left[-\frac{(D_p \alpha_n^2 - S_p)}{(D_p/L_p^2 - S_p)} e^{(x_j/L_p)} + e^{-\alpha_n x_j} \right] + \frac{(D_p \alpha_n^2 - S_p)}{(D_p/L_p^2 - S_p)} e^{(x/L_p)} - e^{-\alpha_n x} \right\} \quad (4)$$

S_p is the recombination rate in the p- type. The positive charge diffusion photon-current equation in the n side, is given by equation,

$$J_n = qD_n \frac{\partial}{\partial x} \delta p \quad (5)$$

By the same way, one can write for electron current density,

$$J_n = q \frac{\phi \alpha_p L_n (1-R)}{\left(\alpha_p^2 L_n - 1\right)} e^{-\left(\alpha_n x_j + \alpha_d W\right)} \times \left\{ \frac{\left(\alpha_p^2 - S_n\right) L_n^2}{\left(D_n - S_n L_n^2\right)} e^{-\alpha_p H'} - 2e^{-\frac{H'}{L_n}} + \alpha_p L_n e^{-\alpha_p H'} \right\} \quad (6)$$

In the same time, the equation of diffusion of the electron current in the p-region is by [22],

$$J_{dr} = q\phi(1-R) e^{-\alpha_n x_j} (1 - e^{-\alpha_d W}) \quad (7)$$

Note that the QE of QD SC is given by [22],

$$QE = \frac{\left(J_p + J_n + J_{dr}\right)}{q\phi(1-R)} \quad (8)$$

NARATIVE OF THE QD SOLAR CELL STRUCTURE

In this research focuses on QE spectrum in TlGaN QDs deposited on GaN which represents as barriers. QDs are implicit in the shape of quantum pointsdisks. The sizes considered are 2 nm in height and 13nm in radius. The structure diagram was exposed in Figure. 1. Parameter of the Material

January-February 2020
ISSN: 0193-4120 Page No. 12952 - 12959

related to TlGaN and GaN QDs are listed in Table 1.

In this research, calculated the the absorption coefficient, and QE to the TlGaN / GaN, where the GaN bulk layer. Good quantum efficiency and the absorption coefficient were obtained for the device, and wide spectrum of wavelength was obtained. It is found, also, that the disk height and the disk radius are 13, 2 nm respectively the bandwidth and QE are high. .High QE can be obtained for structure with TlGaN QD at extensive depth of the junction of the SC device.

ABSORBTION COEFFICIENT OF QUANTUM DOT STRUCTURE

QD absorbs high density of photons with wide spectrum of energies due to randomly distributed and imperfections in shape on the p-type base, which produce an inhomogeneous expansion. The coefficient of absorption by the equation as [14].

$$\alpha(\hbar\omega) = \frac{\pi e^2}{n_b c\varepsilon_\circ m_\circ^2 \omega} \sum_i \int_{-\infty}^{\infty} dE' \left|M_{env}\right|^2 \left|e^{\wedge}.p_{cv}\right|^2 \times D(E') L_g(E', \hbar\omega)$$
$$[f_V(E', F_V) - f_C(E', f_C)] \quad (9)$$

Where ε_0 is the permittivity of space , m_0 is the electron mass, c is the velocity of light in space, ω is the angular frequency of the injected optical signal , n_b is refractive index of the semiconductor , M_{env} is the function of envelop overlap between the QD negative and positive states, and E' is the optical transition energy,. The term $\left|\hat{e}.P_{cv}\right|^2 = \frac{3}{2}(m_0/6)E_p$ which represent the momentum of matrix element for heavy hole ,and effective mass to be transition energy in TE polarization, E_P is the optical matrix of energy parameter. $D(E')$ is the inhomogeneous concentration of states of self-assembled QDs and it is written as [15]

$$D(E') = \frac{s^i}{V_{dot}^{eff}} \frac{1}{\sqrt{2\pi\sigma^2}} \exp\left(\frac{-(E' - E_{\max}^i)^2}{2\sigma^2}\right) \quad (10)$$

Where s^i is the degeneracy at every situation of a QD,. V_{dot}^{eff} is the effective volume for the QDs(Quantum Dotes) , σ is the QDs spectral variance distribution, and $E_{\max}^i$ is the value of energy at the maximum of QD distribution of the i^{th} optical transition. The terms f_c and f_v are the respective quasi-Fermi distribution function for the conduction and valence bands, respectively.

DESCRBING THE QDs SOLAR CELS

In this study QE in TlGaN QDs deposited onGaN as barriers and QDs implicit to be in the shape of quantum disks. The size studied was 2 nm in height and 13 nm a radius. The diagram of special regions in the structure is shown in Fig. 1. The parameter of Material to the TlGaN QDs and GaN barriers are planned in Table 1.

QD SOLAR CELL STRACTURE

The study of this paper focuses on study QE spectra for CdS QDs grown on TIGaN/GaN layers. It is assumed that QEs can be represented as quantum disks that have a variety of sizes (in height and in radius). A graphical diagram for different parts in the structure is stated in Fig. 2. Material parameters ofTIGaN and GaN QDs can be seen in Table 1.

January-February 2020
ISSN: 0193-4120 Page No. 12952 - 12959

Table 1. Parameters considered to determine QE of TlGaN/GaN QD SCs

parameter	Symbol(unit)	TlGaN	GaN
Electron diffusion length	Ln(µm)	$0.33.10^{-6}$	$0.33.10^{-6}$
Hole diffusion length	Lp(µm)	$0.422.10^{-6}$	$0.422.10^{-6}$
Electron carrier lifetime	N nsτ	$0.54.10^{-9}$	$0.54.10^{-9}$
Hole carrier lifetime	P nsτ	$0.054.10^{-9}$	$0.054.10^{-9}$
Depletion width	W µm	$0.98.10^{-6}$	$0.98.10^{-6}$
Junction depth	Xj µm	2.10^{-6}	2.10^{-6}
Superiattice thickness	H µm	2.10^{-6}	2.10^{-6}
Front surface power reflective	R	0.99	0.99
Illumination photon number	Photon/sϕ	10^{8}	10^{8}

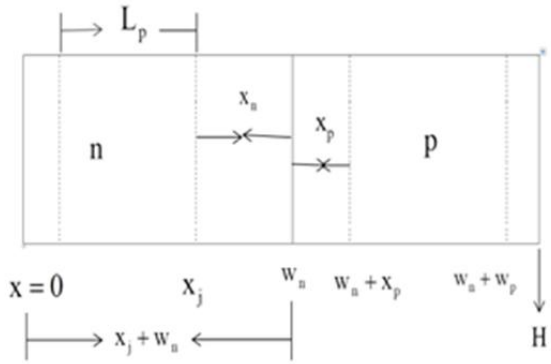

Fig. 2: A graphical diagram of different layers in the structure of QD solar cell.

THE ABSORPTION SPECTRUM OF TIGaN/GaNQD

The absorption spectrum of n-doping (TIGaN/GaN)QD system for both structure dimensions where the height of the disk equal to 2nm and the radius of the disk is 13nm shown in Figure . 1 .It can be seen that It covers the range 380-440nm which lies in the UV,and Visible range . The spectrum covers it was peaked at 410 n*m* wavelength. The peak due to the transition from the 2nd subband . The absorption peak values to be 125000cm-1 at the p-type side .as seen from the Figure . 3 the absorption spectrum for the QD *In TlGa N / TIG* . The absorption increase twice under p-doping (blue curve) and peaked at 410 n*m*.

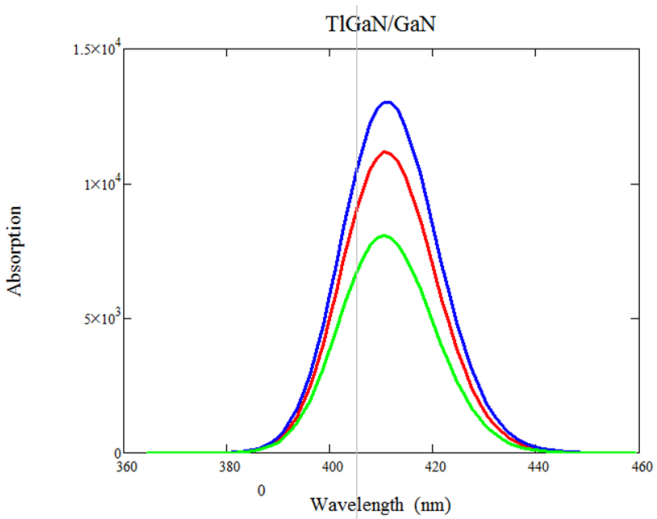

Fig. 3: shows the Absorption for the TIGaN/GaN structure when h=2nm and =13nm.

RESULTS AND DISCUSSION

QE was determined using Eq. (8), for TIGaN/GaN QD SCs structures at the sizes mentioned in section 3

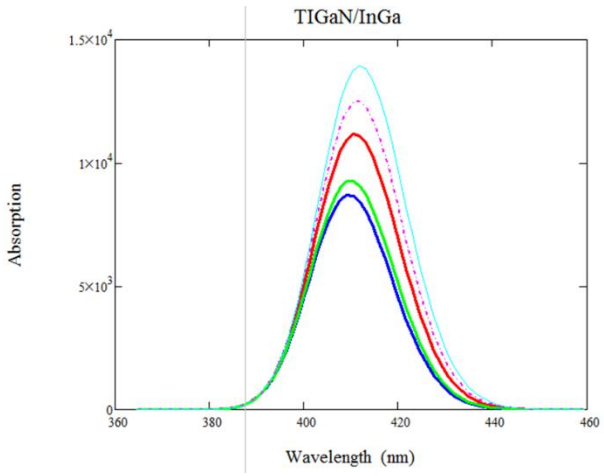

Fig. 4: shows the Absorption for the TIGaN/GaN structure when h=2nm and ρ =13nm.

When h=2nm and ρ=13 nm It can be detected from figure 4 that there is one major peak for each Temperature ; lies at 410 nm ,412 nm,414 nm,416,and 420 nm which correspond to the temperatures 260,270,300,320,and 340 respectively.

January-February 2020
ISSN: 0193-4120 Page No. 12952 - 12959

which can see that there is shift in the peak with increase temperature to word the visible region ,in the same time the absorption intensity increase from lowest value which correspond to least value of temperature and so on increase the absorption intensity with increase temperature due to reduce value of energy gap for the semiconductor .The intensity increase with increase the temperature due to increase the number of distention of exciton and the increase energy of phonons . The main peak comes from the first subband transition ,which represent represent the ground state transition.

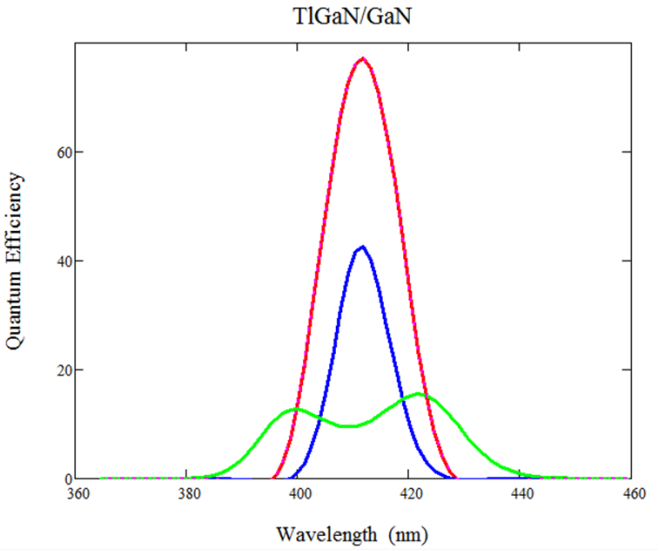

Figure 5 Quantum Efficiency as a function of wavelength

Fig.5QD structure is shown in red line. The most contribution related to absorption in the p-region, which is represented by *QEp*(Red solid line) at the peak and Quantum efficiency are 70 at 412. The contribution of both of the n-doped region QE_n(blue line) ,and the depletion region QE_{dr}(green solid line) are very few. The peak of QE_p appears the same as that of *QEn while* QE_{dr} has two peaks the first one at 395 nm related to ground state transition, and second at 425 nm related to exited state transition. QE peak value approaches 0.73.

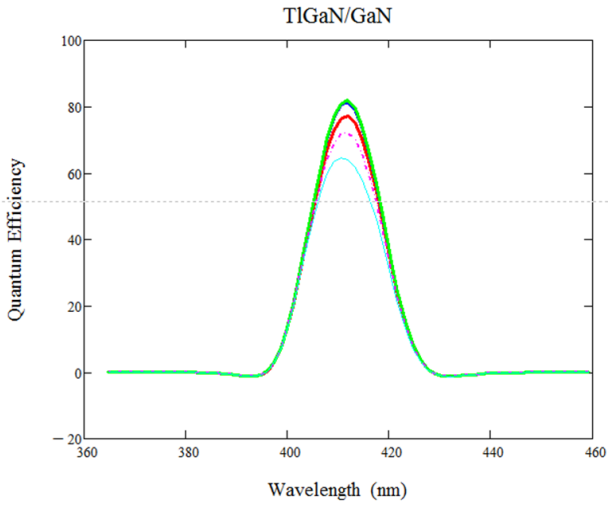

Fig. 6: QE of TIGaN/GaN QD structure at different values of temperature .

Figure 5 explain the relationship between the Quantum efficiency for the device TIGaN/GaN structure .There is one and main peak lies between 390 nm,and 430 nm which represent the spectrum of the device region work for the solar cells ,which has high value of Quantum efficiency .The figure 6 also explain the effect environment temperature on the device of solar cells .one can be seen from the figure that the quantum efficiency increase with increase the temperature where the QE was 60 at 260 K after that increase to 80 at 340 K in the same time there is small shift in the wavelength where the peak at 410 nm at temperature 260 K shift to 416 nm at 340 K which mean the device improved with increase temperature as result of increase the number of excitons destination, and phonon energy with increase the temperature .

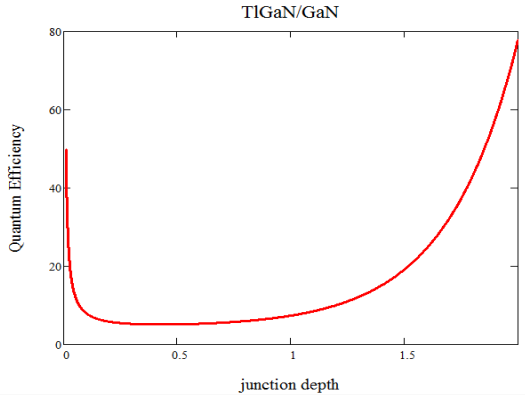

Fig. 7: The quantum efficiency with junction depth of TIGaN/GaN QD structure h=2nm,=13nm. values of hole diffusion length L_n

January-February 2020
ISSN: 0193-4120 Page No. 12952 - 12959

THE JUNCTION DEPTH AS A FUNCTION OF QE

this section focus on QE versus junction depth is plotted as seenfrom the figure 7 the quantum efficiency drop slightly with increase the junction depth till 0.5 then increase the Quantum efficiency with increasing of junction depth exponentially ,which is tuning junction depth to get optimum value of Quantum efficiency .exposed that the electron diffusion length is an efficient in this material giving on obvious discrimination between QE Curves. The separation between curves begins at junction depth.

CONCLUSION:

This research is studying optical absorption, and QE of TIGaN/GaN Quantum dotes solar cells. As a result, the structure of the band was designing to the QDs which in the form the quantum disk shape. Where the absorption spectra, QE have been calculated, and investigated at different Temperature with different junction depths. It is revealed that doping the barrier layer provide low QE but wide bandwidth as in the case of TIGaN. In addition, It is found that increase of the temperature results increase the absorption intensity and Quantum efficiency with shift the peak toward visible spectrum . Good quality QE can obtain for TIGaN/GaN at lengthy depth of the junction of the solar cell structure.

REFERENCES

1. Dakhil, T., Abdulalmuhsin, S. M., & Al-Khursan, A. H. (2018). QE of cadmium sulphide QD photodetectors. Micro & Nano Letters, 13(8), 1185-1187.
2. AbdulAlmohsin, S., & Cui, J. (2012). Graphene-enriched P3HT and porphyrin-modified ZnO nanowire arrays for hybrid solar cell applications. The Journal of Physical Chemistry C, 116(17), 9433-9438.
3. Yamamoto, K., Asahi, H., Fushida, M., Iwata, K., &Gonda, S. (1997). Gas source molecular beam epitaxy growth of TlInP for new infrared optical devices. Journal of applied physics, 81(4), 1704-1707.
4. AbdulAlmohsin, S., Armstrong, J., & Cui, J. (2012). CdSnanocrystal-sensitized solar cells with polyaniline as counter electrode. Journal of Renewable and Sustainable Energy, 4(4), 043108.
5. Chen, A.-B., &Piao, J. (1999). Bandgap Variation and Miscibility Gaps of Thallium-Based Pseudo-Binary Alloys. MRS Online Proceedings Library Archive, 607
6. Tanabe, T., & Nakahara, K. (2004). Semiconductor luminous elements and semiconductor laser: Google Patents.
7. Nejad, S. M., Samani, S., &Rahimi, E. (2010). Characterization of responsivity and quantum efficiency of TiO 2—Based photodetectors doped with Ag nanoparticles. Paper presented at the 2010 2nd International Conference on Mechanical and Electronics Engineering.
8. Shah, K., Lund, J., Olschner, F., Moy, L., &Squillante, M. (1989). Thallium bromide radiation detectors. IEEE Transactions on Nuclear Science, 36(1), 199-202.
9. Zhang, J., Fu, J., Li, F., Xie, E., Xue, D., Mellors, N. J., &Peng, Y. (2012). BaFe12O19 single-particle-chain nanofibers: preparation, characterization, formation principle, and magnetization reversal mechanism. Acs Nano, 6(3), 2273-2280..
10. htomo, A., Kawasaki, M., Koida, T., Masubuchi, K., Koinuma, H., Sakurai, Y., . . . Segawa, Y. (1998). Mg x Zn 1− x O as a II–VI widegap semiconductor alloy. Applied Physics Letters, 72(19), 2466-2468.
11. Pârlog, M., Borderie, B., Rivet, M., Tăbăcaru, G., Chbihi, A., Elouardi, M., . . .Tassan-Got, L. (2002). Response of CsI (Tl) scintillators over a large range in energy and atomic number of ions. Part I: recombination and δ-electrons. Nuclear Instruments and Methods in Physics Research Section A: Accelerators, Spectrometers, Detectors and Associated Equipment, 482(3), 674-692.
12. Dakhil, T., Abdulalmuhsin, S. M., & Al-Khursan, A. H. (2018). Tunable mechanisms of quantum efficiencies in CdSe and TiO 2 quantum dot solar cells. Applied optics, 57(4), 612-619.
13. Dakhil, T., Abdulalmuhsin, S. M., & Al-Khursan, A. H. (2018). QE of cadmium sulphide QD

January-February 2020
ISSN: 0193-4120 Page No. 12952 - 12959

photodetectors. Micro & Nano Letters, 13(8), 1185-1187.

14. Hall, J. F., & Ferguson, W. (1955). Optical properties of cadmium sulfide and zinc sulfide from 0.6 micron to 14 microns. JOSA, 45(9), 714-718.
15. Liu, B., Shakouri, A., & Bowers, J. E. (2002). Wide tunable double ring resonator coupled lasers. IEEE Photonics Technology Letters, 14(5), 600-602.
16. Dwara, S. N., & Al-Khursan, A. H. (2016). Two-window InSbBi quantum-dot photodetector. Applied optics, 55(21), 5591-5595.